Micro-/nanostructured alumina as model surface to study topography effects on cell-surface interactions

Cenk Aktas, Marina Martinez Miró, Juseok Lee, Stefan Brück, Michael Veith, CVD/Biosurfaces Group

Introduction

Cells exhibit highly sensitive interactions with the surrounding chemical and topographical environment [1]. Surface topography with a definite chemistry has been shown to significantly affect cell adhesion, orientation, cell activation and migration [2], but the mechanisms mediating such cell responses still remain unclear. It is an ongoing discussion whether the chemical patterning of the surface is also altered when the topography of the surface is modified. Sherlock et al. demonstrated an improvement of cell adhesion on laser structured polymer surfaces [3]. Similarly, Yu et al. showed alignment of cells on polymer surfaces patterned by laser interference lithography [4]. In such approaches, it is not clear whether the altered surface chemistry or physical patterning influenced the cell interaction with the surface.

In comparison to polymers, ceramics offer better stability in terms of surface chemistry. Alumina has been used as implant material since the early 1970s due to its excellent biocompatibility, corrosion resistance and phase stability [5]. In addition, superior mechanical properties of alumina including high hardness, wear resistance, scratch resistance, low coefficient of friction and sufficient mechanical strength to resist fatigue make it one of the strongest candidates for implant applications among the ceramics [6].

Besides its biocompatibility, the surface topography also plays a crucial role in the performance of alumina implants. In-vitro studies provided evidence of increased osteoblast (bone-forming cell) adhesion on nanophase alumina (e.g. grain sizes less than 100 nm) compared to larger conventional grain size alumina [7]. Such studies demonstrated that enhanced osteoblast adhesion was independent of surface chemistry and the ceramic phase, but was modified by the surface topography. When compared to microscaled ceramic materials, nanoceramics have an increased number of atoms and crystal grains at their surfaces and possess a higher surface area to volume ratio. It has been shown that the cumulative adsorption of proteins from body fluids is significantly higher on smaller, nanometer grain sized materials [8]. Webster et al. correlated enhanced vitronectin adsorption, conformational changes and bioactivity to the increased osteoblast adhesion on nanostructured alumina [9]. Such findings indicate that nanostructures also affect the cellular activities rather than only simply enhancing the surface attachment.

On the other hand, it is known that several cellular processes, such as adhesion, proliferation, migration, differentiation and changes in cell shape, are influenced by the Extracellular Matrix (ECM), which is not only composed of nanostructured features. The ECM consists of various structures at different length scales. For example, specifically for the bone, hydroxyapatite platelets are between 2 and 5 nm in width and 50 nm in length, whereas Type I collagen fibers are a triple helix of 300 nm in length, 0.5 nm in width and have a periodicity of 67 nm [10]. Besides these nanoscaled structures, microscaled features such as macrophages are also found in the ECM. In this context, 3D artificial structures mainly composed of fibrous structures, but also accommodating pores for larger, microscaled features may be of interest for studying cell-surface interactions.

In the current study, we introduce a new approach to prepare nano- to micro-structured alumina surfaces by combining chemical vapor deposition (CVD) and pulsed laser treatment. We synthesized Al/Al_2O_3 biphasic nanowires by the decomposition of

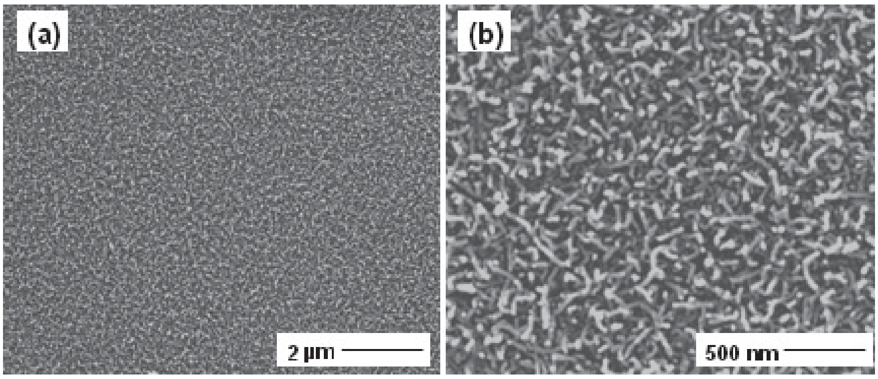

Figure 1: SEM images of deposited nanowires at (a) low magnification and (b) high magnification.

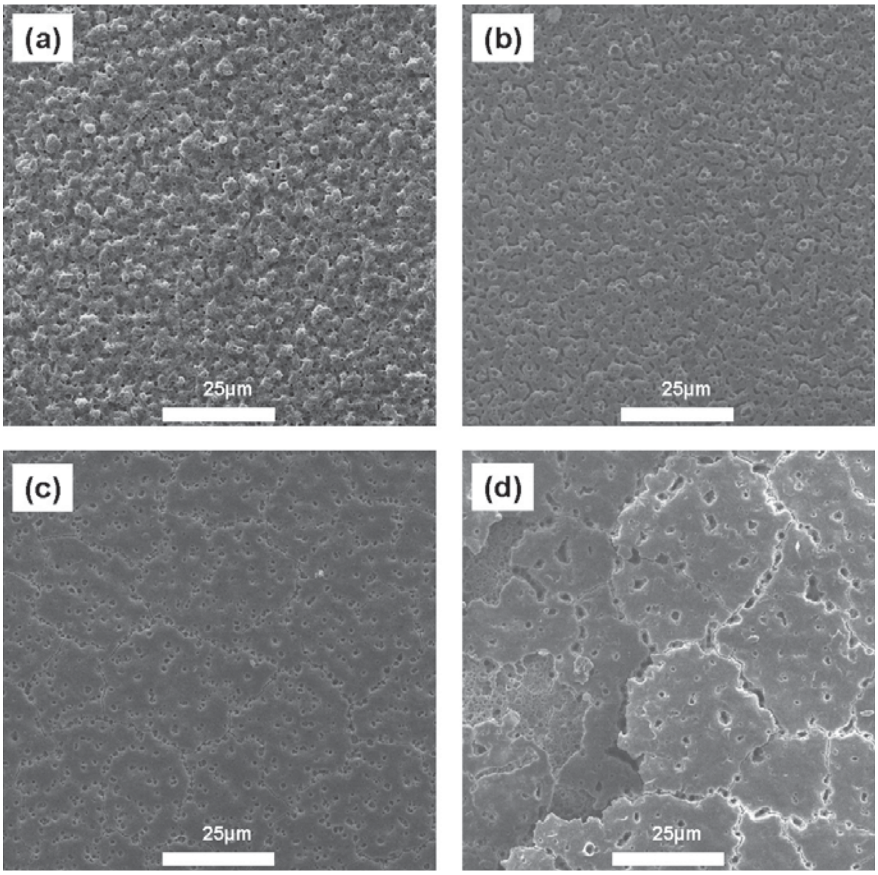

Figure 2: SEM images of the deposited layers after (a) 1 laser pulse, (b) 2 laser pulses, (c) 4 laser pulses and (d) 8 laser pulses.

$(^tBuOAlH_2)_2$ on metal, silicon and glass substrates at 600°C. Heat treatment of the Al/Al_2O_3-nanowires by a high energy nanosecond pulsed laser leads to melting and oxidation of the Al-core. The laser treatment produces a large variety of micro- and nanostructured Al_2O_3 surfaces with identical chemical composition. Depending on the integral laser energy and thus the completion of the oxidation of the Al core, the chemical composition can vary between $Al_{1.0}{\cdot}Al_2O_3$ and $Al_{0.0}{\cdot}Al_2O_3$, which always results in an identical shell. In both cases, Al_2O_3 is the outer chemical compound, which may be responsible for the interaction with cells.

Experimental

Al/Al_2O_3 bi-phasic nanowires were deposited by the decomposition of the single source molecular precursor $(^tBuOAlH_2)_2$ on heated metallic substrates under a reduced pressures of 2-5x10^{-2} mbar. Prior to the deposition, the precursor compound $(^tBuOAlH_2)_2$ was synthesized following the routes described elsewhere [11] under dry N_2 using standard Schlenk techniques.

For laser treatment, we used an Nd:YAG laser which generates laser pulses of 4 to 8 ns, with a maximum pulse energy of 2000 mJ, at a repetition rate of 10 Hz and a fundamental wavelength of 1064 nm. By frequency doubling, a wavelength of 532 nm with maximum pulse energy of 1000 mJ (with a spot size of 8mm) was used for texturing of the deposited layers due to their strong absorption covering UV to NIR wavelengths. The number of laser shots, N, was controlled with an electromechanical shutter. The surface structuring was studied by applying different laser fluencies and numbers of pulses, N.

As-deposited and laser treated samples were visualized by means of SEM (FEI Quanta 400 FEG) at an accelerating voltage of 10 kV. The crystal structure was examined by Raman spectroscopy (Labview Aramis Raman microspectrometer, Horiba Jobin Yvon). The surface composition was analyzed using a PHI 5600 XPS employing monochromatic Al Kα X-rays.

Results and Discussion

Figure 1a and 1b show SEM images of randomly grown Al/Al_2O_3-nanowires on metallic substrates at 600 °C. Recently, we have shown that such bi-phasic nanowires have uniform diameters of about 20-30 nm and are composed of an inner Al-core that is wrapped up by an Al_2O_3-shell at a constant molar ratio of Al/Al_2O_3 = 1:1 [12].

Figure 2 displays SEM images of the surface topography produced by nanosecond laser processing at the near-damage-threshold fluency of F=0.2 J/cm^2 for different numbers of laser pulses. The main features are random nanopores, nanoprotrusions or micro-nano hillocks. After a single laser pulse, the extreme temperature increase induces a local surface melting, as can be seen in Figure 2a. The regions on the surface which are covered with relatively dense and highly interpenetrated nanowires exhibit stronger optical absorption. These regions seem to be partially molten and the molten material has flown over the surface. Micro-grooves and protrusions form due to the fast solidification of the expelled liquid on the boundary of the solid state material. The change in the color of the deposited layers from black to white (not shown here) also shows similarities to the transformation of the Al/Al_2O_3 composite to Al_2O_3 which is similar to our previous observations in case of CW laser treatment [13].

The second laser pulse creates a relatively smooth surface due to re-melting of the layer, as is shown in Figure 2b. The surface becomes smoother after four laser pulses, but it seems likely that repeated thermal shocks create cracks on the surface (Figure 2c). After eight pulses delamination of the film was observed. This is an indication of extremely high thermal shocks. Li et al. [14] and Guo et al. [15] showed similar deformations and delamination of the layers after repeated high energy pulses. Higher magnification SEM micrographs, given in Figure 3, show more hints on the pulsed laser modification of deposited layers.

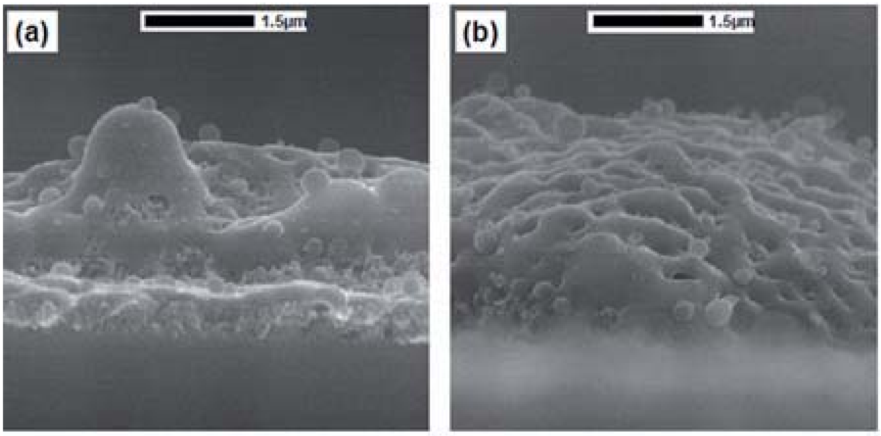

Figure 3a and 3b: SEM images of the deposited layers after a single laser pulse.

When the laser fluency is increased to F=0.3 J/cm^2, nanopores and spherical nanoprotrusions with diameters of 60-90 nm form after a single laser pulse. The examination of the SEM images (Figure 3a and b) suggests the following mechanism for the formation of such nanopores and spherical nanoprotrusions: The nanopores are always accompanied by nearby nanoprotrusions, indicating a nano-scaled material transport to an adjacent site. It can be envisioned that a high temperature gradient induces a radial surface tension gradient which expels the spherical liquid droplets to the periphery of the molten material. This may be the reason for the formation of spherical nanostructures upon solidification.

It has been shown that the molten Al core oxidizes to Al_2O_3 after CW laser treatment and XRD analysis clearly showed the formation α-alumina, as demonstrated before [13]. On the other hand, short laser pulses can only heat a thin layer near the surface. Since a local phase analysis is needed on the surface, micro Raman spectroscopy was performed. Figure

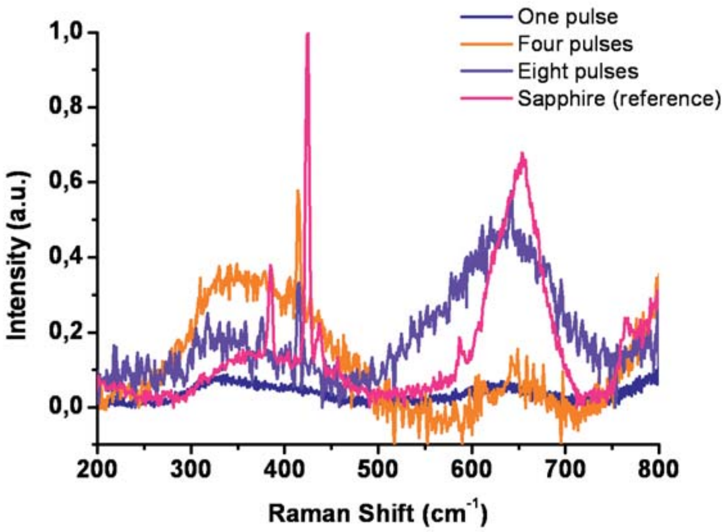

Figure 4: Raman spectra of the deposited layer after various laser pulses and of the sapphire reference.

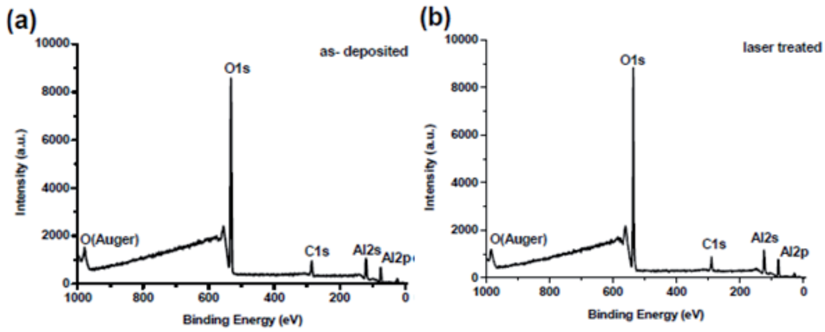

Figure 5: XPS spectra of the deposited layer (a) before and (b) after a single laser pulse.

4 shows the Raman spectra of layers treated with different numbers of laser pulses. For comparison, a reference sapphire sample was also characterized under the same conditions. After the first laser pulse, there is no clear indication of a transformation besides some broad Raman bands which may be due to partial phase transformation to α-alumina. Following the repeated laser pulses, clear α-alumina bands are observed in the spectra, which are comparable with findings of Rena et al. [16].

Figure 5a and 5b show the XPS spectra of the Al/Al_2O_3 layer before and after a single laser pulse. The peaks originate from the ejection of Al 2p, Al 2s, O 1s and C 1s core electrons. In addition, the O (KLL) Auger signals can be easily identified. XPS analysis indicates that the chemical composition of the surface shows no drastic change after the laser treatment. The low carbon content seems to be accumulated during the sample-handling.

Conclusion

Irradiation of deposited nanowires by nanosecond laser pulses in air leads to a melting and oxidation of the Al-core to Al_2O_3. Pulsed laser treatment produced a large variety of microstructures and nanostructures. Such a combination of nano- and microscaled features is important to study cell–surface interactions since the ECM is made of multi-scale features. After repeated laser pulses, a formation of sphere-like microstructures was observed. Besides the variety of surface structures, the chemical state remains identical in each case. Such surfaces are suitable to perform cell culture experiments, revealing a clear influence of the nano- and microtopography on the cell adhesion and proliferation.

References

[1] R. Singhvi, G. Stephanopoulos, D. I. C. Wang; Biotechnol. Bioeng. Mater. 43 (1994), 764.
[2] A. Curtis, C. Wilkinson; Biomaterials 18, 24 (1997).
[3] R. J. Sherlock, D. N. Bhogal, M. Ball, T. J. Glynn; Proc. of SPIE Vol. 4876.
[4] F. Yu, F. Mücklich, P. Li, H. Shen, S. Mathur, C.-M Lehr, U. Bakowsky; Biomacromolecules 6 (2005) 1160-1167.
[5] D. L. Wise, D. J. Trantolo, D. E. Altobelli, M. J. Yaszemski, J. D. Gresser; Human Biomaterials Applications, Humana Press, Totowa, New Jersey (1996).

[6] C. C. Berndt, G. N. Haddadt, A. J. D. Farmer, K. A. Gross; Mater. Forum 14 (1990), 161.
[7] T. J. Webster, R. W. Siegel, R. Bizios; Scr. Mater. 44 (2001), 1639.
[8] E. M. Christenson, K. S. Anseth, J. J. J. P. van den Beucken, C. K. Chan, B. Ercan, J. A. Jansen, C. T. Laurencin, W.-J. Li, R. Murugan, L. S. Nair, S. Ramakrishna, R. S. Tuan, T. J. Webster, A. G. Mikos; J. Orthopaed. Res. 25, 1 (2007), 11.
[9] T. J. Webster, L. S. Schalder, R. W. Siegel, R. Bizios; Mat. Res. Soc. Symp. Proc. 662 (2001).
[10] G.M. Luz, J.F. Mano; Comp. Sci. and Technol. 70 (2010), 1777.
[11] M. Veith, S. Faber, R. Hempelmann, S. Janssen, J. Prewo, H. Eckerlebe; J. Mater. Sci. 31 (1996), 2009.
[12] M. Veith, E. Sow, U. Werner, C. Petersen, C. Aktas; Eur. J. Inorg. Chem. (2008), 5181.
[13] C. Aktas, B. Afrooz, C. Akkan, J. Lee, M. M. Miró, M. Veith; submitted to Materials Letter.
[14] H. Li, S. Costil, V. Barnier, R. Oltra, O. Heintz, C. Coddet; Surf. Coat. Technol. 201 (2006), 1383.
[15] A. Y. Vorobyev, C. Guo; Appl. Surf. Sci. 253 (2007), 7272.
[16] R. Krishnan, R. Kesavamoorthy, S. Dash, A. K. Tyagi, B. Raj; Scripta Materialia 48 (2003), 1099.

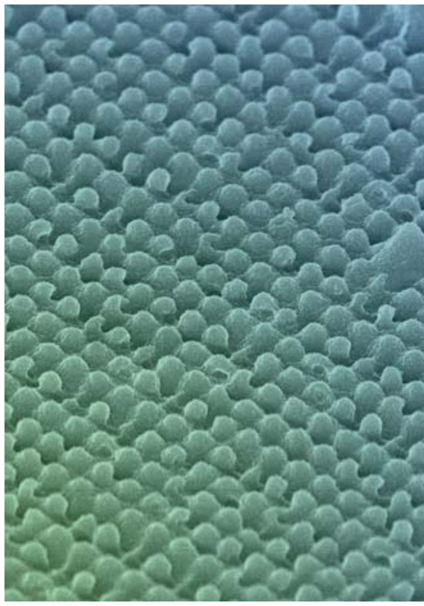

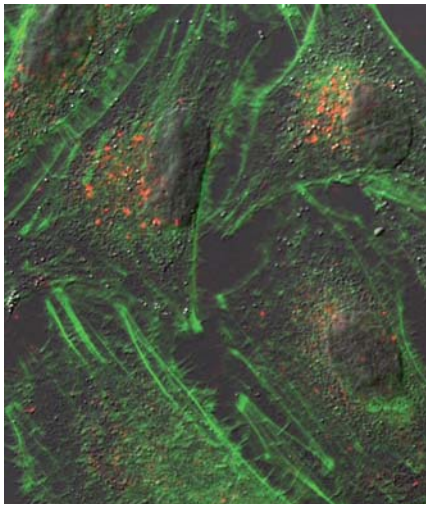

Jahresbericht 2010

Leibniz Gemeinschaft

INM Leibniz-Institut für Neue Materialien